

International Federation of Automatic Control

18th IFAC Workshop on Control Applications of Optimization CAO 2022

Gif sur Yvette, France, 18–22 July 2022

PROCEEDINGS

Edited by
Tatiana Filippova
Russian Academy of Sciences



ELSEVIER

Copyright © 2022 the authors.
Open access publication under the CC-BY-NC-ND License
(<https://creativecommons.org/licenses/by-nc-nd/4.0/>)

IFAC PapersOnline — ISSN 2405-8963

Published by:
International Federation of Automatic Control (IFAC)
Hosting by Elsevier Ltd.

Available online at
www.sciencedirect.com

Publication date
July 2022

Copyright conditions

All publication material submitted for presentation at an IFAC-sponsored meeting (Congress, Symposium, Conference, Workshop) must be original and hence cannot be already published, nor can it be under review elsewhere. The authors take responsibility for the material that has been submitted. IFAC-sponsored conferences will abide by the highest standard of ethical behavior in the review process as explained on the Elsevier webpage (<https://www.elsevier.com/authors/journal-authors/policies-and-ethics>), and the authors will abide by the IFAC publication ethics guidelines (<https://www.ifac-control.org/events/organizers-guide/PublicationEthicsGuidelines.pdf/view>).

Accepted papers that have been presented at an IFAC meeting will be published in the proceedings of the event using the open-access IFAC-PapersOnLine series hosted on [ScienceDirect](https://www.sciencedirect.com/) (<https://www.sciencedirect.com/>). To this end, the author(s) must grant exclusive publishing rights to IFAC under a Creative Commons license when they submit the final version of the paper. The copyright belongs to the authors, who have the right to share the paper in the same terms allowed by the end user license, and retain all patent, trademark and other intellectual property rights (including research data).

(<https://www.ifac-control.org/publications/copyright-conditions>).

18th IFAC Workshop on Control Applications of Optimization — CAO2022

Sponsored by

- International Federation of Automatic Control (IFAC)
- Technical Committee on Optimal Control, TC 2.4

Co-Sponsored by

- IFAC TC 1.2. Adaptive and Learning Systems
- IFAC TC 1.5. Networked Systems
- IFAC TC 2.1. Control Design
- IFAC TC 2.2. Linear Control Systems
- IFAC TC 2.3. Non-Linear Control Systems
- IFAC TC 2.5. Robust Control
- IFAC TC 6.1. Chemical Process Control
- IFAC TC 6.3. Power and Energy Systems
- IFAC TC 6.4. SAFEPROCESS
- IFAC TC 7.1. Automotive Control
- IFAC TC 7.3. Aerospace
- IFAC TC 7.4. Transportation Systems
- IFAC TC 9.4. Control Education



International Program Committee

Fernando Lobo Pereira (PT), Chair
Ilya Kolmanovsky (US), Co-chair
Patrick Panciatici (FR), Co-chair for Industry
Tatiana Filippova (RU), Editor

Tankut Acarman (TR)	Vicenç Puig Cayuela (ES)
Koichi Kobayashi (JP)	Igor Furtat (RU)
Ruth Bars (HU)	Marc Quincampoix (FR)
Alexander Kurzhanski (RU)	Emanuele Garone (BE)
Franco Blanchini (IT)	Davide Raimondo (IT)
Mircea Lazar (NL)	Giulia Giordano (IT)
Julio H. Braslavsky (AU)	Vasso Reppa (NL)
Kwang Y. Lee (US)	Alexandra Grancharova (BG)
Richard D. Braatz (US)	Luis Rodrigues (CA)
Daniel Limón (ES)	Sergio Grammatico (NL)
Jose de Dona (AU)	Noboru Sakamoto (JP)
Dan Ma (CN)	Victoria Grushkovskaya (AT)
Maria do Rosário de Pinho (PT)	Maria Seron (AU)
Carlos Ocampo Martinez (ES)	Lars Grüne (DE)
Stefano Di Cairano (US)	Leonid Shaikhet (IL)
Thulasi Mylvaganam (UK)	Martin Guay (CA)
Natalia Dmitruk (BY)	Hyo-Sang Shin (UK)
Rudy R. Negenborn (NL)	Éva Gyurkovics (HU)
Stefka Fidanova (BG)	Nina N. Subbotina (RU)
Gabriele Pannocchia (IT)	Morten Hovd (NO)
FRsco Ferrante (FR)	Alexander Tarasyev (RU)
Stefan Pickl (DE)	Tor Arne Johansen (NO)
Miroslav Fikar (SK)	Andrezej Turnau (PL)
Boris Polyak (RU)	Marc Jungers (FR)
Rolf Findeisen (DE)	Esteban Vargas (MX)
Jorge Ivan Poveda (US)	Soorathep Kheawhom (TH)
Fernando Fontes (PT)	Vladimir Veliov (AT)
Alexander Poznyak (MX)	Elena Zattoni (IT)
Hélène Frankowska (FR)	

National Organizing Committee

Sorin Olaru (CentraleSupélec), Chair
Ionela Prodan (Grenoble INP), Co-chair
Jean Maeght (RTE), Co-chair for Industry
Sylvain Bertrand (ONERA)
Guillaume Colin (Univ. Orléans)
Estelle Courtial (Univ. Orléans)
Yiping Fang (CentraleSupélec)
Herve Gueguen (CentraleSupélec)
Alessio Iovine (CNRS)
Nicolas Langlois (ESIGELEC)
Maria Makarova (CentraleSupélec)
Laurent Pfeiffer (INRIA)
Pedro Rodriguez (CentraleSupélec)
Serban Sabau (Stevens Institute of Technology)
Cristina Stoica Maniu (CentraleSupélec)
Vincent Talon (Renault)
Sihem Tebbani (CentraleSupélec)
Spilios Theodoulis (TU Delft)
Cristina Vlad (CentraleSupélec)

IFAC-PapersOnline Editorial Board

Editor-in-Chief

Juan A. de la Puente
Universidad Politécnica de Madrid
Spain

Deputy Editor-in-Chief

José-Luis Díez
Universitat Politècnica de Valencia
Spain

Advisor

Carlos Eduardo Pereira
Universidade Federal de
Rio Grande do Sul, Brazil

Editors

Systems and Signals

Hideaki Ishii
Tokyo Inst. of Technology, Japan

Design Methods

Laura Menini
Università di Roma "Tor Vergata",
Italy

Computer, Cognition and Communication

Thierry Marie Guerra
Université de Valenciennes et
Hainaut-Cambrésis, France

Mechatronics, Robotics and Components

Andreas Kugi
TU Wien, Austria

Cyber-Physical Manufacturing Enterprises

Benoit Iung
CRAN, France

Process and Power Systems

Jay H. Lee
KAIST, Republic of Korea

Transportation and Vehicle Systems

Lars Eriksson
Linköping University, Sweden

Bio & Ecological Systems

Ronald van Nooijen
TU Delft, Netherlands

Social Systems

Lawrence (Larry) Stapleton
Waterford Institute of Technology,
Ireland

Associate Editors

Alessandro Chiuso
Università di Padova, Italy

Tiago Roux Oliveira
Universidade Federal do Rio de
Janeiro, Brazil

Carla Seatzu
Università degli Studi di Cagliari

Yilin Mo
Tsinghua University, China

Maurice Heemels
TU Eindhoven, Netherlands

Sergio Galeani
Università di Roma Tor Vergata,
Italy

Silviu-Iulian Niculescu
CNRS-CentraleSupélec, France

Christophe Prieur
Gipsa-lab Grenoble, France

Eric Kerrigan
Imperial College, United Kingdom

Mario Sznajder
Northeastern University, USA

Yann Le Gorrec
ENSMM, France

Birgit Vogel-Heuser
TU München, Germany

Kevin Guelton
Université de Reims, France

Lei Ma
Southwest Jiaotong University,
China

Tsu-Chin Tsao
UCLA, USA

Ivan Petrovic
University of Zagreb, Croatia

Jianhua Zhang
East China University of Science
and Technology, China

Marco Macchi
Politecnico di Milano, Italy

Dmitry Ivanov
Hochschule für Wirtschaft &
Recht Berlin, Germany

Georg Weichhart
PROFACTOR GmbH, Austria

Wei Ren
University of California, Riverside
USA

Rolf Findeisen
Otto-von-Guericke-University
Magdeburg, Germany

Chris Aldrich
Curtin University, Australia

Yrjö Majanne
Tampere University, Finland

Vicenç Puig
Universitat Politècnica de
Catalunya, Spain

Per Tunestal
Lund Institute of Technology,
Sweden

Roberto Galeazzi
Technical University of Denmark

Antonios Tsourdos
Cranfield University,
United Kingdom

Tankut Acarman
Galatasaray Üniversitesi, Turkey

Zdzisław Kowalczyk
Politechnika Gdańska, Poland

Manoj Karkee
Washington State University
USA

Thomas Desaive
University of Liege, Belgium

Marialisa Volta
Università di Brescia, Italy

Alejandro Vargas Casillas
UNAM, Mexico

Fei-Yue Wang
Chinese Academy of Sciences,
China

Mariana Netto
Université Gustave Eiffel, France

Qing-Shan (Samuel) Jia
Tsinghua University, China

Antonio Visioli
Università di Brescia, Italy

Peter Kopacek
TU Vienna, Austria

FOREWORD

The Control Applications of Optimization (CAO) workshop series started in 1979 and reached this year in its 18th edition. It continues its original mission to provide a forum for addressing the latest developments in Optimal Control Theory and the Optimization-based design in automation and decision-making processes. By building on solid and rich System Theory, Control and Optimization pillars, it seeks its perpetual rejuvenation and vitality by embracing the current scientific advances, technological developments and societal challenges, thus ensuring its imperative place in the current and future most daring human endeavors.

CAO 2022 was held in France in the new campus of CentraleSupélec within the University Paris-Saclay. The workshop was held as a hybrid event which encouraged the in-presence participation but didn't penalize the authors from regions still affected by COVID-19 related restrictions on worldwide travel. Moreover, the workshop was held concurrently and in the same location with the 27th International Conference on Difference Equations and Applications (ICDEA 2022). The participants of IFAC CAO 2022 thus had the opportunity to connect with the participants of this major event of the International Society of Difference Equations (ISDE).

In spite of the uncertainty brought about by extraordinary times the world is going through, 98 contributions were submitted and rigorously peer reviewed by 248 researchers. All the papers submitted for regular/invited session received at least two solid reviews, and the vast majority received three reviews. The program committees accepted 72 papers that are published in these proceedings corresponding to the oral contributions presented in 16 sessions of the program.

Special thanks go to our distinguished plenary speakers: Jean-Bernard Lasserre, Angelia Nedich, Tamer Başar and Simona Onori for sharing their research and perspectives and to Yurii Nesterov who provided a Special Key-Note Lecture sponsored by the CentraleSupélec Foundation. The Invited Talk from Industry given by Patrick Panciatici and a panel discussion on the interplay between academic research and industrial applications have nicely complemented the technical program. The workshop was preceded by 3 tutorial sessions and a mini-symposium on constrained control, thus amounting to a one-week immersion in the optimal and optimization-based control topics.

More than 100 participants registered for the conference, with 80% in-person participation. We would like to warmly thank them and all authors whose contributions were critical to the success of the event. We are also deeply grateful to all the people behind the scenes whose work was invaluable to the conference organization: IPC members for their hard work on the construction of the technical content of the workshop, NOC members for managing all the different aspects concerning the organization and the team of volunteers from the Laboratory of Signals and Systems of CentraleSupélec for running of the hybrid sessions and ensuring the success of the social events. Finally, we are deeply grateful to our sponsors and in particular to RTE, through the RTE Chair at CentraleSupélec, for the unwavering support of the event.

Sorin Olaru
(General Chair)

Fernando Lobo Pereira
(IPC Chair)

Ilya Kolmanovsky
(IPC Co-Chair)

Patrick Panciatici
(IPC Co-Chair for Industry)

Ionela Prodan
(NOC Co-Chair)

Jean Maeght
(NOC Co-Chair for Industry)

Tatiana Filippova
(Editor)

Optimal single-interval control for SIR-type systems

A.H. González* A. Ferramosca** E.A. Hernandez-Vargas***

* *Institute of Technological Development for the Chemical Industry (INTEC), CONICET-Universidad Nacional del Litoral (UNL), Santa Fe, Argentina. Email: alejgon@santafe-conicet.gov.ar*

** *Department of Management, Information and Production Engineering, University of Bergamo, Bergamo, Italy*

*** *Instituto de Matemáticas, UNAM, Juriquilla, Mexico*

Abstract: Although modeling studies are focused on the control of SIR-based systems describing epidemic data sets, few of them present a formal dynamic characterization in terms of the two main indexes: the infected peak prevalence (*IPP*) and the final epidemic size (*EFS*). These indices are directly related to equilibrium sets and stability, which are crucial concepts to understand what kind of non-pharmaceutical interventions (social distancing, isolation measures, mask-wearing, etc.) can be implemented to handle an epidemic. The objective of this work is to provide a theoretical single-interval control strategy that simultaneously minimizes the *EFS* while maintaining the *IPP* arbitrary low, according to health system capacity limitations. Several simulations illustrate the true role of the herd immunity threshold and provide new insight into the way authorities may act.

Copyright © 2022 The Authors. This is an open access article under the CC BY-NC-ND license (<https://creativecommons.org/licenses/by-nc-nd/4.0/>)

Keywords: Epidemic Control, Stability Analysis, SIR Systems, single-interval Control

1. INTRODUCTION

SIR-type models are based on the seminal work of Kermack and McKendrick (1927), which firstly established a compartmental relationship between the main variables of an epidemic: Susceptible, Infected and Removed individuals. Surprisingly, even when significant improvements have been made in the general understanding of the SIR dynamics, the core of almost any epidemic behavior is still qualitatively described by the relatively simple original 3-state model. With the outbreak of the novel COVID-19 (produced by the SARS-CoV-2) at the end of 2019, a plethora of studies have been developed to explain how the virus spread around the world: all of them, with more or less complexity, bases their forecast, analysis and control strategies on SIR-type models. In Brauer and Castillo-Chavez (2012) a formal analysis was made concerning the general behaviour of SIR-type models and the limit values (for time going to infinity) of the state variables were characterized for several scenarios and initial conditions corresponding to the outbreak of the epidemic. In Harko et al. (2014) an exact explicit solution for SIR model was given, which allowed the scientific community to go further with a more detailed dynamical analysis. Later on, Franco (2020); Bertozzi et al. (2020) made further analysis concerning the effect of a time varying coefficient with control purposes. SIR-type models are not only useful to understand epidemic behaviors but also (and more important) to assess the ways one can control them according to *a priori* specified objectives. The qualitative evaluation of the different scenarios corresponding to different government measures (social distancing, lockdown, use of face mask, hygiene recommendation, vaccination,

etc.) represents a helpful tool for the authorities decision-making in emergency times. At this point, dynamical and control system theory (Sontag (2013)) becomes crucial to exploit formal mathematical analysis to account for optimal control actions.

From a theoretical control perspective, this problem falls into the classic framework of optimal control (Lewis et al. (2012)) where one obtains the best possible performance (effect) by using the less possible control action (cause) (Sethi and Thompson (2000)). However, in the case of SIR-type systems describing epidemics, the cause-effect separation is not so clear. Many studies have been done to find an optimal-control-based social intervention for SIR models in the context of the current epidemic of COVID-19. The two main metrics to measure the disease impact are (Di Lauro et al. (2021)): the infected peak prevalence, *IPP* (maximal fraction of infected individuals along time), which is closely related to the health systems capacity, and the epidemic final size, *EFS* (total fraction infected). In principle, optimal solutions minimizing either the *EFS* or the *IPP* can be obtained by using a single-interval social distancing (Sadeghi et al. (2020)); i.e., a fixed reduction of the infection rate (and so the reproduction number \mathcal{R}) for a given period. On one hand, Sadeghi et al. (2020); Federico and Ferrari (2020); Morris et al. (2021) make a rigorous analyses to show how to find the optimal single-interval control action that minimizes *IPP*. Even when nice theoretical results are obtained, their main drawback is that they do not account for the other severity index, the *EFS*. Reciprocally, similar results are presented in Bliman and Duprez (2021); Di Lauro et al. (2021); Ketcheson (2020), but minimizing the *EFS*. Again, in addition to

some implementation problems, their main drawback is the disregards of the *IPP*.

The common factor in all the cited literature is that no conclusive results are shown concerning the best single-interval policy to simultaneously minimize the *IPP*, *EFS*. In this article, we show that the key point is to separate transient and stationary regimes. Based on a pure dynamical analysis of the SIR-type models, we do not consider the control objective of minimizing the infected peak prevalence (*IPP*) or the epidemic final size (*EFS*), but we just steer the susceptible to the (open-loop) herd immunity, which is the minimal *EFS* at steady-state for any finite-time intervention. Furthermore, by taking advantage of the fact that the infected peak is independent of the *EFS*, the *IPP* is maintained under an upper bound, computed to account for the health system capacity. As demonstrated by several simulation results, this theoretical strategy seems to be general enough to provide a confidence baseline to policymakers in a pandemic context.

2. CONTROL SIR MODEL

This section reviews the SIR epidemic model Kermack and McKendrick (1927), which describes the fractions of susceptible $S(t)$ and infectious $I(t)$ individuals in a population at time t . Infections occur proportional to $S(t)I(t)$ at a transmission rate β , and infectious individuals are removed (recover or die) at a rate γ . Non-pharmaceutical interventions (mainly social distancing) reduce the transmission rate, $\beta(t)$, below its nominal value, which is fixed. The SIR model can be written in non-dimensional form by rescaling the time ($\tau := t\gamma$) as (Franco (2020)):

$$\dot{S}(\tau) = -\mathcal{R}(\tau)S(\tau)I(\tau), \quad (1a)$$

$$\dot{I}(\tau) = \mathcal{R}(\tau)S(\tau)I(\tau) - I(\tau), \quad (1b)$$

where $\mathcal{R}(\cdot) := \beta(\cdot)/\gamma$ denotes the time-varying reproduction number fulfilling $\mathcal{R}(\cdot) \in \Omega_{\mathcal{R}}$. $\Omega_{\mathcal{R}}$ is the set of single-interval controls:

$$\Omega_{\mathcal{R}} := \{ \mathcal{R}(\cdot) : \mathbb{R}_{\geq 0} \rightarrow \mathbb{R}_{\geq 0} : \mathcal{R}(\tau) = R_{si}, \text{ for } \tau \in [\tau_s, \tau_f], \\ \text{and } \mathcal{R}(\tau) = \bar{\mathcal{R}}, \text{ for } \tau \in [0, \tau_s) \text{ and } \tau \in (\tau_f, \infty) \}, \quad (2)$$

where $R_{si} \in [\underline{\mathcal{R}}, \bar{\mathcal{R}}]$, $0 < \tau_s < \tau_f < \infty$ denote the starting and ending single-interval intervention times ($\tau_f < \infty$ to model the fact that social distancing has always an end), and $0 < \underline{\mathcal{R}} < \bar{\mathcal{R}}$ are the minimal (maximal social distancing) and maximal (non-intervention) values for the reproduction number. The case $\underline{\mathcal{R}} = 0$ is not considered, since a perfect full lockdown is not possible.

Susceptible S and infectious I are constrained to be in the set $\mathcal{X} := \{(S, I) \in \mathbb{R}^2 : S \in [0, 1], I \in [0, 1], S + I \leq 1\}$, for all $\tau \geq 0$. Particularly, denoting $\tau=0$ the epidemic outbreak time, it is assumed that $(S(0), I(0)) := (1 - \epsilon, \epsilon)$, with $0 < \epsilon \ll 1$; *i.e.*, the fraction of susceptible individuals is smaller than, but close to 1, and the fraction of infectious is close to zero.

2.1 Open-loop dynamical analysis

We will assume first that $\mathcal{R}(\tau) \equiv \bar{\mathcal{R}}$, for $\tau \in [0, \infty]$ (no-intervention or open-loop scenario). The solution of (1) for $\tau \geq \tau_0 > 0$ depends on $\bar{\mathcal{R}}$ and the initial conditions $(S(\tau_0), I(\tau_0)) \in \mathcal{X}$. Since $S(\tau) \geq 0$, $I(\tau) \geq 0$, for $\tau \geq \tau_0 > 0$,

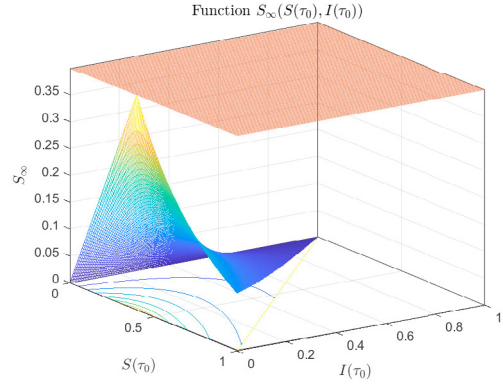


Fig. 1. Function $S_{\infty}(\mathcal{R}, S(\tau_0), I(\tau_0))$ is bounded from above by $S^* = 1/\bar{\mathcal{R}}$ ($S_{\infty} = S^*$, light red plane). Furthermore, S_{∞} reaches its maximum, given by S^* , at $S(\tau_0) = S^*$, $I(\tau_0) = 0$.

then $S(\tau)$ is a decreasing function of τ (by 1.a), for all $\tau \geq \tau_0$. From 1.b, it follows that if $S(\tau_0)\bar{\mathcal{R}} \leq 1$, $\dot{I}(\tau) = (\bar{\mathcal{R}}S(\tau) - 1)I(\tau) \leq 0$ at τ_0 . Furthermore, given that $S(\tau)$ is decreasing, $I(\tau)$ is also decreasing for all $\tau \geq \tau_0$. On the other hand, if $S(\tau_0)\bar{\mathcal{R}} > 1$, $I(\tau)$ initially increases, then reaches a global maximum, and finally decreases to zero. In this case, the peak of I or infected peak prevalence, *IPP*, is reached at $\hat{\tau}$, when $\dot{I} = \bar{\mathcal{R}}SI - I = 0$. *IPP* depends on initial conditions $S(\tau_0)$, $I(\tau_0)$, and $\bar{\mathcal{R}}$, as follows:

$$IPP = I(\tau_0) + S(\tau_0) - (1/\bar{\mathcal{R}})(1 + \ln(S(\tau_0)\bar{\mathcal{R}})). \quad (3)$$

Condition $\dot{I} = \bar{\mathcal{R}}SI - I = 0$ implies that $S = S^*$, where $S^* := \min\{1, 1/\bar{\mathcal{R}}\}$ is a threshold or critical value, known as "herd immunity" (*i.e.*, the value of S under which I cannot longer increase). We define $S_{\infty} := \lim_{\tau \rightarrow \infty} S(\tau)$ and $I_{\infty} := \lim_{\tau \rightarrow \infty} I(\tau)$, which are values that depend on initial conditions $S(\tau_0)$, $I(\tau_0)$, and $\bar{\mathcal{R}}$. By simple calculation we obtain $I_{\infty} = 0$. Furthermore, S_{∞} is given by

$$S_{\infty} := -(1/\bar{\mathcal{R}})W(-\bar{\mathcal{R}}S(\tau_0)e^{-\bar{\mathcal{R}}(S(\tau_0)+I(\tau_0))}). \quad (4)$$

where $W(\cdot)$ is the Lambert function (a detailed analysis of this result can be seen in Abuin et al. (2020), where an analogous in-host model is studied). The epidemic final size, defined as $EFS := 1 - S_{\infty}$, is then given by

$$EFS := 1 + (1/\bar{\mathcal{R}})W(-\bar{\mathcal{R}}S(\tau_0)e^{-\bar{\mathcal{R}}(S(\tau_0)+I(\tau_0))}), \quad (5)$$

which is a function of the initial conditions and $\bar{\mathcal{R}}$.

The following Lemma states the maximum of S_{∞} over \mathcal{X} . *Lemma 1.* (Maximum S_{∞} over \mathcal{X}). Consider system (1) with initial conditions $(S(\tau_0), I(\tau_0)) \in \mathcal{X}$, for some $\tau_0 \geq 0$, and $\bar{\mathcal{R}} > 0$ fixed. Then, the maximum of S_{∞} occurs at $(S^*, 0)$ and it is given by S^* . Furthermore, if $I(\tau_0) \in [\delta, 1]$, for some $\delta > 0$, the maximum takes place at (S^*, δ) and is given by $-W(-\bar{\mathcal{R}}S^*e^{-\bar{\mathcal{R}}(S^*+\delta)})/\bar{\mathcal{R}}$.

Proof. See Appendix A.

Fig. 1 shows S_{∞} for different initial conditions.

2.2 Equilibrium characterization and stability

The equilibrium of system (1), with $\mathcal{R}(\tau) \equiv \bar{\mathcal{R}}$ for $\tau \in [0, \infty]$, is obtained by zeroing each of the differential

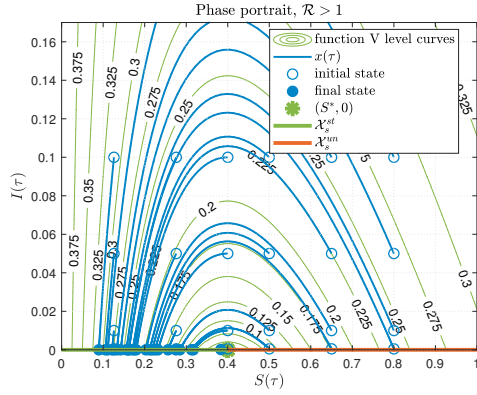


Fig. 2. Phase Portrait for system (1) with $\bar{\mathcal{R}} = 2.9$ and initial conditions $(S(\tau_0), I(\tau_0)) \in \mathcal{X}$. Set \mathcal{X}_s^{st} is in green (thick line), while \mathcal{X}_s^{un} is in red (thick line). Furthermore, the level curves of a Lyapunov function V are plotted (green thin line).

equations. This way, for initial conditions $(S(\tau_0), I(\tau_0)) \in \mathcal{X}$, the equilibrium set is given by $\mathcal{X}_s := \{(\bar{S}, \bar{I}) \in \mathcal{X} : \bar{S} \in [0, S(\tau_0)], \bar{I} = 0\}$, since S is decreasing. Next, a key theorem concerning the asymptotic stability of a subset of \mathcal{X}_s is introduced.

Theorem 2. (Asymptotic Stability). Consider system (1) with $\mathcal{R}(\tau) \equiv \bar{\mathcal{R}}$, constrained by \mathcal{X} . Then, the set $\mathcal{X}_s^{st} := \{(\bar{S}, \bar{I}) \in \mathcal{X} : \bar{S} \in [0, S^*], \bar{I} = 0\}$, where S^* is the herd immunity, is the unique asymptotically stable (AS) set of system (1), with a domain of attraction given by \mathcal{X} .

Proof. See Appendix A.

Fig. 2 shows a Phase Portrait for system (1), with $\bar{\mathcal{R}} > 1$, and $(S(\tau_0), I(\tau_0)) \in \mathcal{X}$.

3. CONTROL STRATEGIES

Non-pharmaceutical interventions are the typical measures that policymakers implement to control epidemics when vaccination is not available. Social distancing, isolation measures, mask wearing, among others, lessens the disease transmission rate $\beta(\tau)$ or, directly, parameter $\mathcal{R}(\tau)$ in system (1). This reduction tends to reduce the two main indexes of the epidemic severity (Di Lauro et al. (2021)): the *IPP* and the *EFS*. Assuming now that $\mathcal{R}(\cdot) \in \Omega_{\mathcal{R}}$ with $\mathcal{R}_{si} \neq \bar{\mathcal{R}}$ (i.e., \mathcal{R} varies over time), *IPP* is no longer given by equation (3). However, equation (5) is still valid to describe the *EFS* (i.e., S_{∞} is still governed by equation (4), given that τ_f is finite). The next Lemma provides an upper bound for S_{∞} when $\mathcal{R}(\cdot) \in \Omega_{\mathcal{R}}$.

Lemma 3. (S steady-state upper bound). Consider system (1) with initial conditions $(S(0), I(0)) = (1 - \epsilon, \epsilon)$, $0 < \epsilon \ll 1$, and $S(0) > S^*$. Consider also that $\mathcal{R}(\cdot) \in \Omega_{\mathcal{R}}$. Then, (i) the system converges to the equilibrium $(S_{\infty}, 0)$ with $S_{\infty} = S_{\infty}(\bar{\mathcal{R}}, S(\tau_f), I(\tau_f))$ bounded from above by S^* , being $S^* < 1$ the herd immunity corresponding to no intervention and, (ii), the only way to achieve $S_{\infty} = S_{\infty}(\bar{\mathcal{R}}, S(\tau_f), I(\tau_f)) \approx S^*$ is with a $\mathcal{R}(\cdot) \in \Omega_{\mathcal{R}}$ producing $S(\tau_f) \approx S^*$ and $I(\tau_f) \approx 0$, which implies that system (1) achieves a Quasi steady-state (QSS) condition at τ_f . Three particularly interesting cases where condition $S_{\infty} \approx S^*$ is not achieved are: (ii.a) if $S(\tau_f) > S^*$ and $I(\tau_f) \approx 0$, then a **second outbreak wave** will occur at some time $\tau > \tau_f$

and, finally, the system will converge to $S_{\infty} < S^*$ (the greater is $S(\tau_f)$ with respect to S^* , the smaller will be S_{∞}), (ii.b) if $S(\tau_f) < S^*$ and $I(\tau_f) \approx 0$, then S_{∞} will be close to $S(\tau_f)$ (the smaller is $S(\tau_f)$ with respect to S^* , the smaller will be S_{∞}), and (ii.c) if $I(\tau_f)$ does not approach zero (i.e., no QSS condition is reached at τ_f), then no matter which value $S(\tau_f)$ takes, S_{∞} will be smaller than S^* (the farther is $S(\tau_f)$ from S^* from above or from below, the smaller will be S_{∞}).

Proof. See Appendix A.

Lemma 3 provides interesting insights into the general dynamic of controlled SIR systems. On one hand, it establishes that the minimal possible *EFS* is exclusively determined by the non controlled epidemic (the value of $\bar{\mathcal{R}}$) and, on the other, it establishes that S^* must be reached as a QSS condition (i.e., with $I(\tau_f) \approx 0$).

Example 1. We simulate (throughout the work) the system (1), with $\bar{\mathcal{R}} = 2.9$ ($\beta = 0.29$ days $^{-1}$ and $\gamma = 0.1$ days $^{-1}$), $I(0) = 1.49 \times 10^{-5}$, $S(0) = 1 - I(0)$ and $\underline{\mathcal{R}} = 0.66$ (Bliman and Duprez (2021)), to demonstrate the main results. Fig. 3 shows the phase portraits under different single-interval control strategies. On the left, two controls $\mathcal{R}(\cdot) \in \Omega_{\mathcal{R}}$ are applied (one strong, with \mathcal{R}_{si} small, and the other soft, with \mathcal{R}_{si} large) at some time τ_s , being $S(\tau_s) = 0.9$ and $I(\tau_s) = 0.07$, up to a large enough time τ_f , such that the system reaches a QSS. In the first case (blue line) $I(\tau_f) \approx 0$ and $S(\tau_f) = 0.7$. Given that $S(\tau_f)$ is significantly greater than $S^* = 0.35$ and $I(\tau_f)$ is small but positive, a second wave occurs (which explains the dynamic experienced when hard interventions are implemented for a long period of time), that drives S_{∞} to a value significantly smaller than S^* ($S_{\infty} = 0.13$). In the second case (red line), $I(\tau_f) \approx 0$ and $S(\tau_f) = 0.15$. Since $S(\tau_f)$ is significantly smaller than S^* , and it cannot longer grow for $\tau > \tau_f$, so S_{∞} is again significantly smaller than S^* ($S_{\infty} = 0.15$). The key point is that τ_f is finite, so the state evolves in open-loop behavior for $\tau > \tau_f$. This can be seen by considering the level curves of a Lyapunov function for the open-loop system (green lines), which encircles the equilibrium $(S^*, 0)$. These curves are invariant trajectories for the open-loop system, so once the system reaches one of them at τ_f , it will continue on the same curve for all $\tau > \tau_f$, in such a way that outer states at τ_f correspond to outer states for $\tau \rightarrow \infty$. In Fig. 3 (right), the same two controls are applied at the same time τ_s , but they are interrupted at a finite time τ_f such that the system has not reached a QSS condition. In the first case (blue line) the state evolution is such that $S(\tau_f) = 0.8$ and $I(\tau_f) = 0.05$. Then, for $\tau > \tau_f$, the system goes along one level curve of the Lyapunov function, which steers the system to $(S_{\infty}, I_{\infty}) \approx (0.09, 0)$, with S_{∞} significantly smaller than S^* . In the second case (red line), $S(\tau_f) = 0.49$ and $I(\tau_f) = 0.2$. This way, the corresponding level curve of the Lyapunov function drives the system - again - to $(S_{\infty}, I_{\infty}) \approx (0.09, 0)$, with S_{∞} significantly smaller than S^* , showing that any control action interrupted before a QSS is reached will necessarily produce a steady-state with S_{∞} smaller than S^* .

3.1 Control objective, redefined

Once the maximal for S_{∞} (minimal for the *EFS*) is established, the question is whether or not it is possible

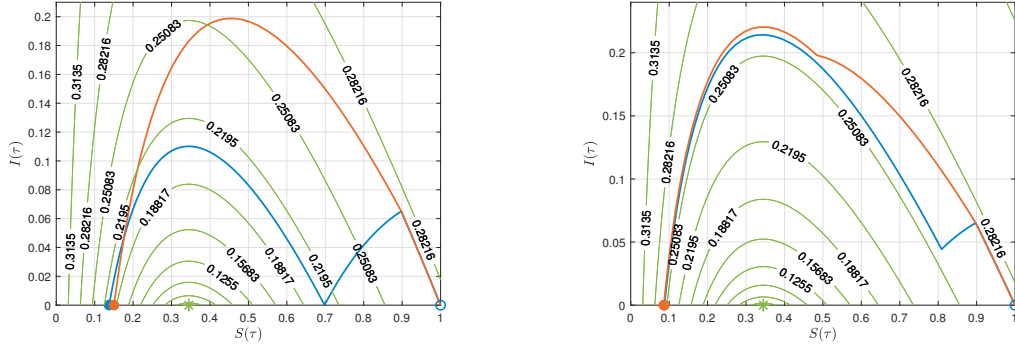


Fig. 3. Long term (left) and short term (right) single-interval control phase portrait. Initial state: empty circle, (S_∞, I_∞) : filled circles, level curves of the Lyapunov function $V(S, I) := S - S^* - S^* \ln(\frac{S}{S^*}) + I$; green lines. No matter which control $\mathcal{R}(\cdot) \in \Omega_{\mathcal{R}}$ is applied, if it is interrupted at a finite τ_f and the system has not reach a QSS condition $(S(\tau_f), I(\tau_f)) \approx (S^*, 0)$, condition $S_\infty \approx S^*$ will not be achieved.

to arbitrarily reduce the *IPP*, while maintaining $S_\infty \approx S^*$. To have a first insight into the answer, consider the integral of equation (1).b, $I(\tau) = \int_0^\tau \mathcal{R}(t)S(t)I(t)dt - \int_0^\tau I(t)dt + c$, where c is a constant determined by the initial conditions $S(0)$ and $I(0)$. Then, $\int_0^\tau I(t)dt = \int_0^\tau \mathcal{R}(t)S(t)I(t)dt - I(\tau) = -S(\tau) - I(\tau) + c$, and taking $\tau=0$, it follows that $c = S(0) + I(0) = 1 - \epsilon + \epsilon = 1$. Now, considering the limits for $\tau \rightarrow \infty$, and recalling that $\mathcal{R}(\tau) \equiv \bar{\mathcal{R}}$ for $\tau \in (\tau_f, \infty)$, it follows that $\int_0^\infty I(t)dt = 1 - S_\infty - I_\infty = 1 - S_\infty$. This latter equality means that, even when \mathcal{R} varies over time, S_∞ only determines the area under the curve of $I(\tau)$, $AUC_I := \int_0^\infty I(t)dt$, but not its peak *IPP*. In other words, it is possible to minimize the *EFS* and also keep the *IPP* under a maximal value imposed by the health system capacity, as long as $\int_0^\infty I(t)dt = 1 - S^*$.

Remark 4. It is not right for an optimal control strategy to simply minimize $\int_0^\infty I(t)dt$, as it is often done, since the minimum is already given by $1 - S^*$. Such a selection leads to unnecessary competition between steady-state objectives (minimize the *EFS*) and transient ones (minimize the *IPP* by minimizing I), which necessarily produces an intermediate solution that optimizes neither *EFS* nor *IPP*.

In this work, we propose to pose the control objective in a rather different way.

Definition 5. Consider system (1) with initial conditions $(S(0), I(0)) = (1 - \epsilon, \epsilon)$, $0 < \epsilon \ll 1$, and $S(0) > S^*$. Consider also that $\mathcal{R}(\cdot) \in \Omega_{\mathcal{R}}$, and that a maximal value for I , $I_{max} > 0$, is established according to the health system capacity. Then, the **epidemiological control objective** consists of steering $S(\tau)$ to S^* , as $\tau \rightarrow \infty$ ($EFS \approx 1 - S^*$), while $IPP \leq I_{max}$.

4. GOLDILOCKS SINGLE-INTERVAL INTERVENTION

We now face the fundamental challenge of finding some $\mathcal{R}(\cdot) \in \Omega_{\mathcal{R}}$ that fulfills the control objective of Definition 5. By making $S_\infty(\mathcal{R}_{si}^*, S(\tau_s), I(\tau_s)) = S^*$, for a specific $\mathcal{R}_{si}^* \in [\underline{\mathcal{R}}, \bar{\mathcal{R}}]$, we have

$$\mathcal{R}_{si}^*(S^*, S(\tau_s), I(\tau_s)) := \frac{\ln S(\tau_s) - \ln S^*}{S(\tau_s) + I(\tau_s) - S^*}. \quad (6)$$

Given that system (1) evolves in open-loop before τ_s , then $(S(\tau_s), I(\tau_s))$ are determined by the (unique) solution of

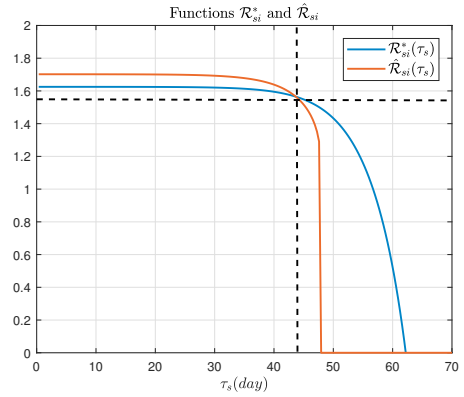


Fig. 4. Functions $\mathcal{R}_{si}^*(S^*, \tau_s)$ and $\hat{\mathcal{R}}_{si}(I_{max}, \tau_s)$, for $\bar{\mathcal{R}} = 2.9$ and $I_{max} = 0.1$. Both reproduction numbers coincides at $\tau_s^g = 43.71$ days, where $\mathcal{R}_{si}^g = 1.57$

the system (1) under the effect of $\bar{\mathcal{R}}$. So we can write $\mathcal{R}_{si}^*(S^*, \tau_s)$ to emphasize the dependence of \mathcal{R}_{si}^* on τ_s . Indeed, for a given S^* , $\mathcal{R}_{si}^*(S^*, \tau_s)$ is a decreasing function of τ_s , as it is shown in Fig. 4, blue line. Furthermore, $\mathcal{R}_{si}^*(S^*, 0) \approx -\frac{\ln S^*}{1 - S^*}$ (given that $S(0) \approx 1$ and $I(0) \approx 0$) and $\mathcal{R}_{si}^*(S^*, \hat{\tau}) = \frac{\ln S^* - \ln S^*}{S^* + IPP - S^*} = 0$, since once the open-loop S evolution reaches S^* at $\hat{\tau}$, with a high value of $IPP(\bar{\mathcal{R}}, S(\tau_0), I(\tau_0)) = I(\hat{\tau})$, nothing can be done to reach the condition $S_\infty \approx S^*$.

Now we define another specific $\hat{\mathcal{R}}_{si} \in [\underline{\mathcal{R}}, \bar{\mathcal{R}}]$ that guarantees $I(\tau) \leq I_{max}$, for all $\tau \in \mathbb{R}_{\geq 0}$. By making $IPP(\hat{\mathcal{R}}_{si}, S(\tau_s), I(\tau_s)) = I_{max}$, we obtain the implicit function

$$\hat{\mathcal{R}}_{si} = \hat{\mathcal{R}}_{si}(I_{max}, \tau_s). \quad (7)$$

For a given I_{max} , $\hat{\mathcal{R}}_{si}(I_{max}, \tau_s)$ is a decreasing function of τ_s , as shown in Fig. 4, red line.

Finally, by merging the latter two conditions, it is possible to define a (so-called) goldilocks intervention:

Definition 6. The **goldilocks single-interval intervention** is defined by a starting time, τ_s^g , fulfilling condition $\mathcal{R}_{si}^*(S^*, \tau_s^g) = \hat{\mathcal{R}}_{si}(I_{max}, \tau_s^g)$, and the fixed reproduction number value, $\mathcal{R}_{si}^g := \mathcal{R}_{si}^*(S^*, \tau_s^g) = \hat{\mathcal{R}}_{si}(I_{max}, \tau_s^g)$.

The goldilocks single-interval intervention allows us to establish the following Theorem:

Theorem 7. Consider system (1) with initial conditions $(S(0), I(0)) = (1 - \epsilon, \epsilon)$, $0 < \epsilon \ll 1$, and $S(0) > S^*$. Consider that $\mathcal{R}(\cdot) \in \Omega_{\mathcal{R}}$ and consider a given I_{max} . Then, if for S^* and I_{max} there exists a goldilocks single-interval intervention, it is the only one that arbitrarily approaches the epidemiological control objectives, as $\tau_f \rightarrow \infty$.

Proof. See Appendix A.

Example 2. Now we evaluate the goldilocks single-interval intervention by resuming the *Example 1*. Consider $I_{max} = 0.1$ and $S^* = 0.35$. In Fig. 4 shows the intervention starting time and reproduction number correspond to the goldilocks scenario ($\tau_s^g = 43.71$ days and $\mathcal{R}_{si}^g = 1.57$, respectively). Fig. 5 (left), shows $S(\tau)$ (blue, upper plot), $I(\tau)$ (red, upper plot) and $\mathcal{R}(\tau)$ (lower plot) for a period of time of 300 days. On the other hand, Fig. 5 (right) shows the corresponding phase portrait, and the level curves of Lyapunov functions, V^* (green curves) and V^g (red curves), corresponding to $\bar{\mathcal{R}}$ and \mathcal{R}_{si}^g , respectively. The level curves of V^g cross that of V^* and, given that $\mathcal{R}_{si}^g < \bar{\mathcal{R}}$, there is one that 'guides' the system exactly to $(S^*, 0)$. This level curve is the one picked by the goldilocks single-interval intervention, applied at τ_s^g .

5. CONCLUSION

In this work, the infected peak prevalence and the epidemic final of SIR-type models were characterized and, based on this characterization, concrete epidemiological objectives involving both indexes were defined. It is shown that a single-interval control - denoted goldilocks control - is able to accomplish with this control objective, at least theoretically. The next step toward a more realistic control problem is to propose a proper optimal controller able to account for realistic scenarios.

REFERENCES

- Abuin, P., Anderson, A., Ferramosca, A., Hernandez-Vargas, E.A., and Gonzalez, A.H. (2020). Characterization of sars-cov-2 dynamics in the host. *Annual reviews in control*.
- Bertozzi, A.L., Franco, E., Mohler, G., Short, M.B., and Sledge, D. (2020). The challenges of modeling and forecasting the spread of covid-19. *Proceedings of the National Academy of Sciences*, 117(29), 16732–16738.
- Bliman, P.A. and Duprez, M. (2021). How best can finite-time social distancing reduce epidemic final size? *Journal of theoretical biology*, 511, 110557.
- Brauer, F. and Castillo-Chavez, C. (2012). *Mathematical models for communicable diseases*. SIAM.
- Di Lauro, F., Kiss, I.Z., and Miller, J.C. (2021). Optimal timing of one-shot interventions for epidemic control. *PLOS Computational Biology*, 17(3), e1008763.
- Federico, S. and Ferrari, G. (2020). Taming the spread of an epidemic by lockdown policies. *Journal of Mathematical Economics*, 102453.
- Franco, E. (2020). A feedback sir (fsir) model highlights advantages and limitations of infection-based social distancing. *arXiv preprint arXiv:2004.13216*.
- Harko, T., Lobo, F.S., and Mak, M. (2014). Exact analytical solutions of the susceptible-infected-recovered (sir) epidemic model and of the sir model with equal death

and birth rates. *Applied Mathematics and Computation*, 236, 184–194.

- Kermack, W.O. and McKendrick, A.G. (1927). A contribution to the mathematical theory of epidemics. *Proceedings of the royal society of london. Series A, Containing papers of a mathematical and physical character*, 115(772), 700–721.
- Ketcheson, D.I. (2020). Optimal control of an sir epidemic through finite-time non-pharmaceutical intervention. *arXiv preprint arXiv:2004.08848*.
- Lewis, F.L., Vrabie, D., and Syrmos, V.L. (2012). *Optimal control*. John Wiley & Sons.
- Morris, D.H., Rossine, F.W., Plotkin, J.B., and Levin, S.A. (2021). Optimal, near-optimal, and robust epidemic control. *Communications Physics*, 4(1), 1–8.
- Sadeghi, M., Greene, J., and Sontag, E. (2020). Universal features of epidemic models under social distancing guidelines. *bioRxiv*.
- Sethi, S.P. and Thompson, G.L. (2000). *What is optimal control theory?* Springer.
- Sontag, E.D. (2013). *Mathematical control theory: deterministic finite dimensional systems*, volume 6. Springer Science & Business Media.

Appendix A. PROOFS

Proof of Lemma 1. Denote $S(\tau_0) = S$, $I(\tau_0) = I$ and $\mathcal{R} = \bar{\mathcal{R}}$. Define $S_{\infty}^{op}(\delta) := \max_{S,I} \{S_{\infty} : (S, I) \in \mathcal{E}(\delta)\}$, where $\mathcal{E}(\delta) := \{(S, I) \in \mathbb{R}^2 : S \in [0, 1], I \in [\delta, 1]\}$ is a set of initial conditions with $I \geq \delta$, for some fixed $\delta \in [0, 1]$. Define also the maximizer initial conditions as $(S^{op}(\delta), I^{op}(\delta)) := \arg \max_{S,I} \{S_{\infty} : (S, I) \in \mathcal{E}\}$. We will show that $S_{\infty}^{op}(\delta) = -W(-\mathcal{R}S^*e^{-\mathcal{R}(S^*+\delta)})/\mathcal{R}$, $(S^{op}(\delta), I^{op}(\delta)) = (S^*, \delta)$ and, particularly, that $S_{\infty}^{op} := S_{\infty}^{op}(0) = S^*$, being S^* the herd immunity.

According to (4), S_{∞} is given by $S_{\infty} := -W(-f(\mathcal{R}, S, I))/\mathcal{R}$, with $f(\mathcal{R}, S, I) := \mathcal{R}S e^{-\mathcal{R}(S+I)}$. Given that $-W(-x)$ is an increasing (injective) function of $x \in [0, 1/e]$ and \mathcal{R} is fixed, then S_{∞} achieves its maximum over $\mathcal{E}(\delta)$ at the same values of S and I as $f(\mathcal{R}, S, I)$ (next it is shown that $f(\mathcal{R}, S, I) \in [0, 1/e]$ for all $(S, I) \in \mathcal{E}(\delta)$ and $\delta \in [0, 1]$). Then, we focus the attention in finding the maximum (and the maximizing variables) of $f(\mathcal{R}, S, I)$. Let denotes the maximum of f as $f^{op}(\delta) := \max_{S,I} \{f(S, I) : (S, I) \in \mathcal{E}(\delta)\}$, while the maximizing variables are $S^{op}(\delta)$ and $I^{op}(\delta)$. Given that the maximum of f occurs at the minimal values of I , let us consider, for simplicity, that $g(S, I) = I - \delta$, in such a way that we want to solve $(S^{op}(\delta), I^{op}(\delta)) = \arg \max_{S,I} \{f(\mathcal{R}, S, I) : g(S, I) \leq 0\}$ (we ignore the conditions $0 \leq S \leq 1$ and $I \leq 1$, but it is easy to see the no maximum is achieved at the boundaries of these constraints). Then $\nabla f = [\frac{\partial f}{\partial S}, \frac{\partial f}{\partial I}] = [\mathcal{R}e^{-\mathcal{R}(S+I)}(1 - \mathcal{R}S), \mathcal{R}^2 S e^{-\mathcal{R}(S+I)}]$ and $\nabla g = [\frac{\partial g}{\partial S}, \frac{\partial g}{\partial I}] = [0, 1]$. Optimality conditions can be written as $\nabla f = \lambda \nabla g$, where $\lambda \in \mathbb{R}_{\geq 0}$ is a Lagrange multiplier. Then, $[\mathcal{R}e^{-\mathcal{R}(S^{op}(\delta)+I^{op}(\delta))}(1 - \mathcal{R}S^{op}(\delta)), \mathcal{R}^2 S^{op}(\delta) e^{-\mathcal{R}(S^{op}(\delta)+I^{op}(\delta))}] = [0, \lambda]$, which implies that $\mathcal{R}e^{-\mathcal{R}(S^{op}(\delta)+I^{op}(\delta))}(1 - \mathcal{R}S^{op}(\delta)) = 0$ and $\mathcal{R}^2 S^{op}(\delta) e^{-\mathcal{R}(S^{op}(\delta)+I^{op}(\delta))} = \lambda$. Since $\mathcal{R} > 0$, the first equality implies that $1 - \mathcal{R}S^{op}(\delta) = 0$, or $S^{op}(\delta) = \min\{1/\mathcal{R}\} = S^*$ (since $S^{op}(\delta) \in [0, 1]$). This way, the second equality reads $\mathcal{R}^2 S^* e^{-\mathcal{R}(S^*+I^{op}(\delta))} = \lambda$, which is true for any value

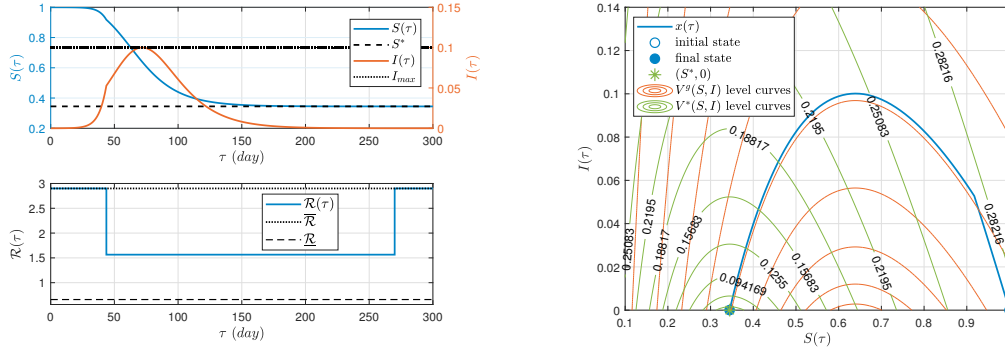


Fig. 5. S, V and \mathcal{R} time evolution, (left), and phase portrait, (right). System with $S^* = 0.35$ and $I_{max} = 0.1$, when the goldilocks single-interval intervention is applied. The indexes are: $EFS = 0.66$, $IPP = 0.10$.

of $I^{op}(\delta) \in [\delta, 1]$ and $\lambda > 0$. As we know that larger values of f are achieved for smaller values of I , then, $I^{op}(\delta) = \delta$. The maximum of S_∞ is then given by $S_\infty^{op}(\delta) = S_\infty(S^{op}(\delta), I^{op}(\delta))$, which reads $S_\infty^{op}(\delta) = -W(-\mathcal{R}S_\infty^{op}(\delta)e^{-\mathcal{R}(S_\infty^{op}(\delta)+I^{op}(\delta))})/\mathcal{R} = -W(-\mathcal{R}S^*e^{-\mathcal{R}(S^*+\delta)})/\mathcal{R}$. If $\mathcal{R} \geq 1$, then $\mathcal{R}S^* = 1$, and so $S_\infty^{op}(\delta) = -W(-e^{-\mathcal{R}(S^*+\delta)})/\mathcal{R}$. On the other hand, if $\mathcal{R} < 1$, then $\mathcal{R}S^* = \mathcal{R}$ and $S_\infty^{op}(\delta) = -W(-\mathcal{R}e^{-\mathcal{R}(S^*+\delta)})/\mathcal{R}$. Particularly, $S_\infty^{op} := S_\infty^{op}(0) = -W(-e^{-1})/\mathcal{R} = 1/\mathcal{R} = S^*$, if $\mathcal{R} \geq 1$, and $S_\infty^{op}(0) = -W(-\mathcal{R}e^{-\mathcal{R}})/\mathcal{R} = \mathcal{R}/\mathcal{R} = 1 = S^*$, if $\mathcal{R} < 1$. \square

Proof of Theorem 2. The proof is divided into two parts. First it is shown that \mathcal{X}_s^{st} is the smallest attractive equilibrium set in \mathcal{X} . Then, it is shown that \mathcal{X}_s^{st} is the largest locally $\epsilon - \delta$ stable equilibrium set in \mathcal{X} which, together with the previous results, implies that \mathcal{X}_s^{st} is the unique asymptotically stable (AS) of system (1), with a domain of attraction (DOA) given by \mathcal{X} .

Attractivity: Consider equation (4). Since $W(z)$ is an increasing function (it goes from -1 at $z = -1/e$ to 0 at $z = 0$), it reaches its minimum at $z = -1/e$. $z(S(\tau_0), I(\tau_0)) = -\mathcal{R}S(\tau_0)e^{-\mathcal{R}(S(\tau_0)+I(\tau_0))}$ reaches its maximum when $S(\tau_0) = S^*$, independently of the values of \mathcal{R} and $I(\tau_0)$ (see Lemmas 1), in which case it is $z(S(\tau_0), I(\tau_0)) = 1/e$. Then, $W(z)$ is bounded from above by -1 , which means that S^* is an upper bound for S_∞ . Therefore, $S_\infty \in [0, S^*]$, which shows the attractivity of \mathcal{X}_s^{st} . Fig. 1 shows a plot of S_∞ as a function of $S(\tau_0)$ and $I(\tau_0)$ for a fixed value of $\mathcal{R} > 1$ (a similar plot can be obtained for $\mathcal{R} < 1$, in which S_∞ reaches its maximum at the vertex of the domain, $S(\tau_0) = 1$ and $I(\tau_0) = 0$). To show that \mathcal{X}_s^{st} is the smallest attractive set in \mathcal{X} , consider a state $(\bar{S}, \bar{I}) := \bar{x} \in \mathcal{X}_s^{st}$ and an arbitrary small ball of radius $\epsilon > 0$, w.r.t. \mathcal{X} , around it, $\mathbb{B}_\epsilon(\bar{x}) \in \mathcal{X}$. Pick two arbitrary initial states $x_{0,1} = (S_{0,1}, I_{0,1})$ and $x_{0,2} = (S_{0,2}, I_{0,2})$ in $\mathbb{B}_\epsilon(\bar{x})$, such that $S_{0,1} \neq S_{0,2}$. These two states converge, according to equation (4), to $x_{\infty,1} = (S_{\infty,1}, 0)$ and $x_{\infty,2} = (S_{\infty,2}, 0)$, respectively, with $S_{\infty,1}, S_{\infty,2} \in [0, S^*]$. Given that function $z(S(\tau_0), I(\tau_0))$ is monotone (injective) in $S(\tau_0)$ and $I(\tau_0)$, and $W(z)$ is monotone (injective) in z , then $S_{\infty,1} \neq S_{\infty,2}$. This means that, although both initial states converge to some state in \mathcal{X}_s^{st} , they necessarily converge to different points. Therefore neither single states $\bar{x} \in \mathcal{X}_s^{st}$ nor subsets of \mathcal{X}_s^{st} are attractive in \mathcal{X} , which shows that \mathcal{X}_s^{st} is the smallest attractive set in \mathcal{X} .

Local $\epsilon - \delta$ stability: Let us consider an equilibrium point $\bar{x} := (\bar{S}, 0)$, with $\bar{S} \in [0, S^*]$ (i.e., $\bar{x} \in \mathcal{X}_s^{st}$). Then a Lyapunov

function candidate is given by $V(x) := S - \bar{S} - \bar{S} \ln(\frac{S}{\bar{S}}) + I$. This function is continuous in \mathcal{X} , is positive definite for all non-negative $x \neq \bar{x}$ and, furthermore, $V(\bar{x}) = 0$. Function V evaluated at the solutions of system (1) reads:

$$\begin{aligned} \frac{\partial V(x(\tau))}{\partial \tau} &= \frac{\partial V}{\partial x} \dot{x}(\tau) = \begin{bmatrix} \frac{dV}{dS} & \frac{dV}{dI} \end{bmatrix} \begin{bmatrix} -\mathcal{R}S(\tau)I(\tau) \\ \mathcal{R}S(\tau)I(\tau) - I(\tau) \end{bmatrix} \\ &= \left[\left(1 - \frac{\bar{S}}{S(\tau)}\right) 1 \right] \begin{bmatrix} -\mathcal{R}S(\tau)I(\tau) \\ \mathcal{R}S(\tau)I(\tau) - I(\tau) \end{bmatrix} = I(\tau)(\mathcal{R}\bar{S} - 1) \end{aligned} \quad (A.1)$$

for $x(0) \in \mathcal{X}$ and $\tau \geq 0$. Function $\dot{V}(x(\tau))$ depends on $x(\tau)$ only through $I(\tau)$. So, independently of the value of the parameter \bar{S} , $\dot{V}(x(\tau)) = 0$ for $I(\tau) \equiv 0$. This means that for any single $x(0) \in \mathcal{X}_s$, $I(0) = 0$ and so, $I(\tau) = 0$, for all $\tau \geq 0$. So $\dot{V}(x(\tau))$ is null for any $x(0) \in \mathcal{X}_s$ (i.e., it is not only null for $x(0) = \bar{x}$ but for any $x(0) \in \mathcal{X}_s$). On the other hand, for $x(0) \notin \mathcal{X}_s$, function $\dot{V}(x(t))$ is negative, zero or positive, depending on if the parameter \bar{S} is smaller, equal or greater than $S^* = \min\{1, 1/\mathcal{R}\}$, respectively, and this holds for all $x(0) \in \mathcal{X}$ and $\tau \geq 0$. So, for any $\bar{x} \in \mathcal{X}_s^{st}$, $\dot{V}(x(\tau)) \leq 0$ (particularly, for $\bar{x} = (\bar{S}, 0) = (S^*, 0)$, $\dot{V}(x(\tau)) = 0$, for all $x(0) \in \mathcal{X}$ and $\tau \geq 0$) which means that each $\bar{x} \in \mathcal{X}_s^{st}$ is locally $\epsilon - \delta$ stable. Then, if every state in \mathcal{X}_s^{st} is locally $\epsilon - \delta$ stable, the whole set \mathcal{X}_s^{st} is locally $\epsilon - \delta$ stable. Finally, by following similar steps, it can be shown that \mathcal{X}_s^{un} is not $\epsilon - \delta$ stable, which implies that \mathcal{X}_s^{st} is also the largest locally $\epsilon - \delta$ stable set in \mathcal{X} , which completes the proof. \square

Proof of Lemma 3. The proof of (i) follows from Lemma 1, by replacing $(S(\tau_0), I(\tau_0))$ by $(S(\tau_f), I(\tau_f))$, and the fact that the final intervention time, τ_f , is finite. The proof of (ii) follows from Lemma 1, and the stability analysis made in Theorem 2, applied at $(S^*, 0)$. \square

Proof of Theorem 7. Consider that, for S^* and I_{max} coming from the Control Objective, it there exists some τ_s for which $\hat{\mathcal{R}}_{si} = \hat{\mathcal{R}}_{si}(I_{max}, \tau_s) = \mathcal{R}_{si}^*(S^*, \tau_s)$. Then, by the definition of $\hat{\mathcal{R}}_{si}(I_{max}, \tau_s)$, it follows that $IPP(\hat{\mathcal{R}}_{si}, S(\tau_s), I(\tau_s)) = I_{max}$, which means that $I(\tau) \leq I_{max}$ for all $\tau > 0$. Furthermore, by the definition of $\mathcal{R}_{si}^*(S^*, \tau_s)$ it follows that, for a large enough τ_f , $S(\tau_f)$ arbitrarily approaches S^* while $I(\tau_f)$ approaches 0. Then, by the stability results at $(S^*, 0)$, it follows that states $(S(\tau_f), I(\tau_f))$ arbitrarily close to $(S^*, 0)$ (from above), produce states $(S(\tau), I(\tau))$ arbitrarily close to $(S^*, 0)$ (from below), for $\tau > \tau_f$. Particularly, $S_\infty \approx S^*$. \square